

# Preparation and *in-vitro* evaluation of Paclitaxel-loaded sericin nanoparticles planned for pulmonary drug delivery system

Mustafa EGLA<sup>1</sup>, Nawal A. RAJAB<sup>2\*</sup>

<sup>1</sup> University of Al-Turath, School of Pharmacy, Department of Pharmaceutics, Baghdad, Iraq

<sup>2</sup> University of Baghdad, School of Pharmacy, Department of Pharmaceutics, Baghdad, Iraq

---

## ABSTRACT

One of the most popular and successful antineoplastic drugs, Paclitaxel (PTX), comes from natural sources and is distinguished by its high lipophilicity. Sericin is a naturally occurring hydrophilic protein which become a popular choice for creating scaffolds for tissue engineering or drug delivery systems using nanocarriers. This work aimed to create and analyze sericin nanoparticles loaded with PTX to deliver lung drugs which synthesized utilizing a desolvation technique and were extensively analyzed to determine their physicochemical features, including particle size, Polydispersity index (PDI), entrapment efficiency, zeta potential, and *in vitro* drug release profile. Additionally, *in vitro* aerosolization were conducted to assess the effectiveness of aerosolization and the possibility of delivering drugs to the lungs using PTX-loaded sericin nanoparticles. Cytotoxicity research was performed on these nanoparticles using the A-549 lung cell line. The findings indicated that the sericin nanoparticles loaded with PTX had appropriate particle size, negative zeta potential, high entrapment efficiency, prolonged drug release behavior, and compelling aerosolization features. Moreover, the cytotoxicity assays on cancer cells demonstrated that the sericin nanoparticles loaded with PTX had anticancer solid properties. In conclusion, the PTX-loaded sericin nanoparticles that have been produced show significant potential as an innovative pulmonary drug delivery system for cancer treatment.

---

\*Corresponding author: Nawal A. RAJAB

E-mail: dr.nawalayash@copharm.uobaghdad.edu.iq

ORCID's:

Mustafa EGLA: 0009-0009-7033-283X

Nawal A. RAJAB: 0000-0003-1812-2244

(Received 19 Apr 2024, Accepted 15 Aug 2024)

**Keywords:** Paclitaxel, sericin, protein nanoparticles, aerosols, pulmonary drug delivery system

---

## INTRODUCTION

Lung cancer is the first leading cause of cancer-related deaths worldwide, with an estimated 1.79 million deaths (18% of total deaths due to cancer in 2020). It is also the second most frequent type of malignancy, with more than 2.21 million cases, 11.4% of cancer cases, diagnosed annually. Small and non-small cell lung cancer (NSCLC) are the two types of lung cancer; NSCLC makes up 80–85% of all lung cancer cases<sup>1</sup>.

Currently available conventional treatment methods include immunotherapy, chemotherapy, radiation, and surgery. Chemotherapy is a key treatment strategy for metastatic lung malignancies, helping to manage symptoms and increase patient survival. The cornerstone of chemotherapy for lung cancer is the intravenous delivery of chemotherapeutic drug<sup>2</sup>.

Anticancer medications cause systemic toxicity, which includes nausea, vomiting, hair loss, and fatigue, as well as ineffective drug accumulation at tumorous sites and undesirable distributions in normal organs. Systemic drug administration eventually kills both cancerous and nearby healthy cells (lacks targeting capability)<sup>3</sup>. As a result, creating a treatment plan that can maximize effectiveness while reducing systemic adverse effects is imperative.

Nebulization is a method of delivering medication directly to the lungs through inhaling a fine mist. This method has been shown to be effective in treating a variety of respiratory diseases, including asthma, chronic obstructive pulmonary disease (COPD), and cystic fibrosis. Nebulization is also being investigated as a potential method for delivering chemotherapy drugs to the lungs in the treatment of lung cancer<sup>4</sup>.

Because of its tailored administration and lower risk of systemic adverse effects, inhaled chemotherapy is seen to be a very promising treatment for non-small cell lung cancer. The advantage of using inhaled chemotherapy originate from the usage of a lower amount of the therapeutic agents which despite of that provide a high drug concentration at the cancerous cells which minimize the side effects of these agents because a lower concentration of antineoplastic drugs reaches the systemic circulation in comparison with other routes of drug administration like oral or IV routes. Lastly, compared to intravenous injection, it might also improve the patient's compliance<sup>5</sup>.

One of the most popular and successful antineoplastic drugs, Paclitaxel (PTX), comes from natural sources and is distinguished by its high lipophilicity. It is a pseudoalkaloid whose nucleus is a taxane ring. By blocking the microtubule depolymerization of free tubulins, PTX's anti-proliferative mechanism is utilized to treat a variety of tumors, including ovarian, breast, prostate, and non-small cell lung cancer (NSCLC). Research has demonstrated that PTX suppresses the migration, proliferation, and release of collagenase associated with angiogenesis<sup>6</sup>.

Because of their high drug loading capacity, stability *in vitro* or *in vivo*, controlled release, and ability to maximize the availability of the drug at its intended site of action for therapeutic benefit, nanocarriers are a class of drug delivery systems that have the potential to minimize the degradation of therapeutic agents. They have also attracted much attention in the field of tumor therapy. When a medication is administered to the site of therapeutic action, often smaller doses are required to get clinically effective results<sup>7</sup>.

Safety concerns are a top priority when creating innovative drug delivery systems for the inhalation route. For a drug to be delivered locally through inhalation, excipients included in the composition of an inhaled formulation must be well-tolerated by the respiratory system<sup>8</sup>.

Natural polymers have garnered interest as viable materials for nanocarriers due to their superior biocompatibility, *in vivo* biodegradability, and plentiful renewable supplies<sup>9</sup>.

A naturally occurring hydrophilic protein called sericin is extracted from silkworm cocoons. Its excellent biocompatibility with cells and tissues, biodegradability, lack of immunogenicity, and variety of bioactivities have made it a popular choice for creating scaffolds for tissue engineering or drug delivery systems using nanocarriers<sup>10</sup>.

This study aimed to develop self-assembled PTX-loaded sericin nanoparticles (NPs) made from protein sericin and poloxamer 407 by the modified desolvation method. Poloxamer 407 is self-assembled as a hydrophobic core (PPG) loaded with paclit and a hydrophilic corona made from Pconjugated dates to the hydrophilic protein (sericin). The formulated nanoparticles were then evaluated for their feasibility as carriers for the pulmonary delivery of PTX.

## METHODOLOGY

Paclitaxel and sericin (lyophilized) were procured from Wuhan Senwayer Century Chemical Co., China. Dialysis membrane M.wt. 100 kDa was procured from HiMedia laboratories in Mumbai, India. Dimethylsulfoxide (DMSO) and methanol were procured from BDH Chemicals, Ltd., Liverpool, England. Poloxamer 407 was procured from Sigma-Aldrich, Germany.

### Analytical quantification of PTX using HPLC

PTX's Quantification was determined by an HPLC method adapted from reference<sup>8</sup>. The chromatographic system (SIL-20A HPLC, Shimadzu, Japan) included an autosampler, a variable wavelength detector, and a quaternary pump. Shim-pack VP-ODS column C18 (5  $\mu$ m, 250 mm x 6 mm) (Shimadzu, Japan) was used for the separations. The ultrapure water/acetonitrile (47:53 v/v) mobile phase was supplied at a 1.0 mL/min flow rate. At 227 nm, the Quantification was carried out. PTX produced a six-point standard curve between 25 and 1000 ng/mL, used for Quantification within a validated standard curve. The detection and quantification limits were 6.0 ng/mL and 11.0 g/mL, respectively, based on the linear regression value of  $R^2 = 0.999$ .

### Preparation of PTX-loaded sericin NPs

PTX-loaded sericin NPs were prepared according to the previously reported procedure with modifications. Briefly, sericin powder, poloxamer 407, and PTX were dissolved in 1mL of DMSO at a final concentration of 1, 4.5, and 0.6% (w/v), respectively. The three materials were wholly dissolved using a bath sonicator for 15 min. Subsequently, the resultant solution mixture was added dropwise to 10 mL of deionized water under stirring at 1000 rpm using a magnetic stirrer (Vision Scientific, Korea), permitting the construction of PTX-loaded sericin NPs by self-assembly. Using cellulose dialysis tubes, the resulting NP suspension has been dialyzed against deionized water (100 kDa for 72 h, with frequent changes of deionized water every 4–6 h), allowing the formation of SNPs by self-assembly<sup>11</sup>.

### Particle size/ polydispersity index analysis

The particle size and PDI of PTX-loaded sericin NPs was measured using the dynamic light scattering (DLS) method (Zetasizer, Malvern, UK). The particle size and PDI of one milliliter of each preparation was measured using the Zetasizer. We used quartz cuvettes and set the instrument refractive index at 1.33. The temperature was 25°C, and the scattering angle was 90°. We conducted the experiments three times<sup>12</sup>.

## Measurement of zeta potential

The surface charge of the chosen NP formulation was calculated in terms of zeta potential by calculating their electrophoretic mobility. A Malvern instrument (Zetasizer, Malvern, UK) connected to a laser Doppler anemometer conducted the measurement. The instrument used a scattering angle of 90°<sup>13</sup>. We performed each test three times in the experiments.

## Assessment of entrapment efficiency (EE%)

To determine the EE% of the generated self-assembled NP formulations, we combined 1 mL of NP suspension with 9 mL of methanol and sonicated it for 5 min using a bath sonicator (Powersonic 410, Hwashin Technology, Korea). This is considered “the actual drug content,” determined by the HPLC method described earlier. In addition, we determined “the entrapped drug” by taking another 1 mL of the NP suspension and subjecting it to ultra-centrifugation for 60 min at 20,000 RPM at four °C using a cooling centrifuge (Eppendorf AG, Germany). The remaining supernatant was thrown away; then the remainder was dissolved in 10 mL of methanol and sonicated for 5 min in a bath sonicator to determine the amount of entrapped PTX using the HPLC method described earlier<sup>14</sup>. We performed all tests in triplicate. The EE% of each formulation was calculated using the equation below:

$$EE\% = \frac{\text{Amount of entrapped drug}}{\text{Actual drug content}} \times 100$$

## Transmission electron microscopy (TEM)

The diluted sample was stained with phospho-tungstic acid, dropped on a copper grid, dried at 60°C, and then loaded onto the TEM holder to be imaged with a TEM detector (Joel JEM 1230; Tokyo, Japan). A clean petri dish with a copper grid hexagonal 200-mesh was attached to carbon tape for TEM examination<sup>15</sup>.

## In-vitro release study

The *in-vitro* drug release performance of PTX from self-assembled sericin-based PTX NPs was investigated using the dialysis technique. In summary, a previously soaked dialysis bag was filled with 1 mL of NP dispersion, equivalent to 0.5 mg of PTX (the molecular weight cutoff was 8.0 to 14 kDa). After being hermetically sealed, the dialysis bag was incubated at 37 ± 0.5°C with moderate shaking (100 rpm) in 75 mL of acetate buffer (pH = 5.4) containing brij-35 (0.5% w/v). Two mL of the media were removed at each scheduled time and replaced with freshly released media that had been pre-warmed to 37°C. Centrifuging the extracted release medium for 15 min at 12,000 rpm was done. The supernatant was collected for analysis using the HPLC method described earlier<sup>16</sup>.

The release of marketed PTX (Abraxane®) and free PTX was performed as follows: 10 mg of lyophilized powder was dispersed in 2 mL deionized water, and from this suspension 1 mL (equal to 0.5 mg of PTX) was placed in a dialysis bag, and one the release same as the colloidal dispersion of NPs. For free PTX, 5 mg was dispersed in 10 mL deionized water; from this suspension, 1 mL was taken and placed in the dialysis bag as in the method described for colloidal dispersion NPs and marketed product. The formula used to determine the release rate was  $RR\% = (W_i/W_{\text{total}}) \times 100\%$ , where  $W_i$  is the quantity of PTX measured at the given time, and  $W_{\text{total}}$  is the entire amount of PTX loaded in the dialysis bag. A similarity factor ( $f_2$ ) was used to statistically verify the data obtained from the two release profiles using the equation below:

$$f_2 = 50 \cdot \log\left\{100 \cdot \left[1 + \frac{1}{n} \sum_{t=1}^n (R_t - T_t)^2\right]^{-0.5}\right\}$$

Where ( $n$ ) is the number of dissolution time points. ( $R_t$ ) Moreover, ( $T_t$ ) are the reference (Abraxane® or free drug) and test (PTX loaded sericin NPs) release values at time  $t$ , respectively. The two release profiles are considered similar when  $f_2$  values are greater than 50 (50–100); otherwise, the profiles are not similar<sup>17</sup>.

### **Attenuated total reflectance infrared spectroscopy (ATR-FTIR)**

The drug's compatibility with the excipients was validated by ATR-FTIR (Shimadzu). An IR Affinity-1S spectrophotometer with an ATR accessory was used to determine the spectra of pure PTX, excipients, a 1:1:1 physical combination (PTX: sericin: poloxamer 407), and the optimum formulation. FTIR/ATR spectra [ $4000\text{--}600\text{ cm}^{-1}$ ] were collected with a resolution of  $4\text{ cm}^{-1}$  by co-adding 256 scans for each spectrum at room temperature<sup>18</sup>.

### **Differential scanning calorimeter (DSC)**

The thermal behavior and thermotropic properties of pure PTX, poloxamer 407, pure sericin, and PTX-loaded sericin NPs (lyophilized) were evaluated using differential scanning calorimetry (DSC/TA-60 instrument from Shimadzu, Japan), equipped with the intercooler two cooling system. Nitrogen was utilized as a blank gas, and samples weighing 3-5 mg were heated in aluminum pans with scanning temperatures ranging from  $50\text{--}250^\circ\text{C}$  at a scanning rate of  $10^\circ\text{C}$  per minute<sup>19</sup>.

### ***In-vitro* aerosol dispersion performance by the Next Generation Impactor™ (NGI)**

By US Pharmacopeia (USP) Chapter <601> specifications on aerosols<sup>20</sup>, the *in vitro* aerosol dispersion properties of PTX loaded sericin NPs were determined

using (NGI) (M170 NGI: MSP Corporation, Shoreview, MN, USA) equipped with a stainless-steel induction port (USP throat), which used to connect the device to nebulizer reservoir (Omron NE-U780, Omron Healthcare UK Ltd, UK) through a customized rubber mouthpiece and equipped. Seven specialized stainless steel insert cups are included with the NGI. The NGI was linked to a Copley HCP5 vacuum pump via a Copley TPK 2000 critical flow controller, and a Copley DFM 2000 flow meter (Copley Scientific, UK) was used to measure and modify the airflow rate,  $Q$ , before each experiment<sup>21</sup>. Tween 80 was applied to every cup's particle collecting surface to guarantee effective particle capture and avoid inter-stage losses brought on by particle bounce. In order to do this, each of the eight NGI collection cups was submerged in an ethanol solution containing 1% Tween 80. The coated cups were then put under the fume hood to evaporate the ethanol thoroughly<sup>22</sup>.

For the NGI flow rate of 60 L/min, the effective cutoff diameters for each impaction stage were calibrated by the manufacturer and stated as Stage 1 (8.06  $\mu\text{m}$ ), Stage 2 (4.46  $\mu\text{m}$ ); Stage 3 (2.82  $\mu\text{m}$ ); Stage 4 (1.66  $\mu\text{m}$ ); Stage 5 (0.94  $\mu\text{m}$ ); Stage 6 (0.55  $\mu\text{m}$ ); and Stage 7 (0.34  $\mu\text{m}$ )<sup>23</sup>.

The aerosolization starts by placing 2 ml of NP suspension (equivalent to 1 mg PTX) in a nebulizer cup and nebulizing for 10 min (according to European and Indian guidelines)<sup>24,25</sup> at 25°C, 65% relative humidity, and 60 L/min flow rate.

Each stage of the NGI, the induction port, and the nebulizer device were rinsed with 10 mL of the respective HPLC mobile phase and collected for quantitative analysis by HPLC<sup>26</sup>. The experiment was done in triplicate ( $n=3$ ), and data are represented as mean  $\pm$  SD. The mass median aerodynamic diameter (MMAD), geometric standard deviation (GSD), fine particle fraction (FPF), respirable fraction (RF), and emitted dose (ED) were using CITDAS software (Version 3)<sup>27</sup>.

The fine particle fraction (FPF), respirable fraction (RF), and emitted dose (ED) were calculated as follows<sup>28</sup>.

$$FPF\% = \frac{\text{Mass deposited on stage 2 through stage 7}}{\text{Initial mass loaded in nebulizer}} \times 100$$

$$RF\% = \frac{\text{Mass deposited on stage 2 through stage 7}}{\text{Initial mass on all stages}} \times 100$$

$$ED\% = \frac{\text{Mass recoverd from NGI}}{\text{Initial mass in nebulizer}} \times 100$$

## ***In vitro* cytotoxicity assay**

The antitumor activity of Paclitaxel before and after loading with sericin-based NPs as well as blank NPs was performed by the Central laboratory in the Al-Mustansiriya University using the following procedures.

### **Cell culture**

Human lung adenocarcinoma cell line A-549 was obtained from the American Type Culture Collection (ATCC). The cells were grown as monolayers in RPMI 1640 medium, supplemented with 10% FBS, 100 IU/mL penicillin, and 100 µg/mL streptomycin sulfate at 37°C with 5% CO<sub>2</sub> under fully humidified conditions<sup>29</sup>.

### **MTT assay**

A-549 cells were seeded in 96-well plates at a density of 5000 viable cells per well and incubated for 24 h to allow cell attachment. After 24 h of incubation at 37°C with 5% CO<sub>2</sub>, the growth medium was replaced with 100 µL medium containing either free PTX solution in DMSO, PTX-loaded sericin NPs, or blank NPs (same amount as PTX-loaded sericin NPs) equivalent to PTX concentrations ranging from 0.1, 0.3, 0.5, 1.0, 3.0, 5.0, 10.0, and 30.0 nM of PTX to each well then incubated at 37°C for 72 h. After 72 h of incubation with each compound, 20.0 µL of the MTT (3-(4, 5-dimethylthiazolyl)-2, 5-diphenyltetrazolium bromide) dye (MTT was dissolved in phosphate-buffered saline (PBS) at 5.0 mg/mL) 180 µL of fresh growth medium were added to each 96-well then kept in an incubator for four h at 37°C for the formation of formazan crystals. After incubation, MTT was aspirated off, and DMSO (100 µL) was added to each well to dissolve the formazan crystals after mild shaking for 15 min. The absorbance of the soluble formazan dye was measured at 570 nm using a microplate reader. Absorbance was measured at 570 nm using a microplate reader. Untreated cells were taken as control with 100% viability, and cells without the addition of MTT were used as blanks to calibrate the spectrophotometer to zero absorbance<sup>30, 31</sup>.

### **Statistical analysis**

The experiment's results were reported as the mean ± standard deviation (SD). The samples were analyzed using one-way analysis of variance (ANOVA) to see if there was a significant difference between studied formulations at a significance threshold of  $p < 0.05$ <sup>31</sup>.



## RESULTS AND DISCUSSION

### Preparation and characterization of the prepared NPs

The desolvation and accompanying dialysis procedures were used to create NPs. During the desolvation process, adding a DMSO mixture containing PTX, poloxamer 407, and protein sericin into the aqueous phase caused fast miscibility of DMSO with water, and then NPs were synthesized by spontaneous self-assembly. Paclitaxel was successfully incorporated into the core of self-assembled nanoparticles composed from hydrophobic (poly PPG) copolymers of poloxamer 407, as shown in Figure 1, which highlights the TEM of PTX-loaded sericin NPs. TEM confirms the spherical morphology of NPs, absence of particle aggregation, and core-shell structure. The particles appeared to be solid in structure with rounded outlines (i.e., hydrophobic core presumably containing PTX and a hydrophilic corona (poly PEG) to which hydrophilic protein is conjugated physically); this assumption is the same putative structure proposed by researchers Mandal et al.<sup>11</sup>. Because the corona-forming PEG chain block offers steric protection against non-specific absorption by the phagocytic system and permits prolonged residence in the lung, this is particularly advantageous for local delivery to the lung<sup>32</sup>. The size of formulated PTX-loaded sericin NPs was 145.0 nm with nearly homogeneous and uniform particle distribution in solvent without any aggregation (PDI of 0.25). The EE% of PTX-loaded sericin NPs was 82%.

Zeta potential measurements can determine the stability of a system by assessing the surface charges on particles. Large zeta potential values in absolute numbers often denote more stable systems. PTX-loaded sericin NPs in this study have a zeta potential of  $-30.16 \pm 3.9$  mV, suggesting that it has enough surface charge to be stable. Since the polypropylene oxide and polyethylene oxide segments in Poloxamer 407's structure were both nonionic, the presence of the protein sericin should cause the shift in the NPs' surface charge. The sericin structure has several negatively charged functional groups generated from various amino acid residues. The deprotonation of these carboxylate groups, which results in COO<sup>-</sup> groups, gave PTX-loaded sericin NPs their negative charge<sup>33</sup>.

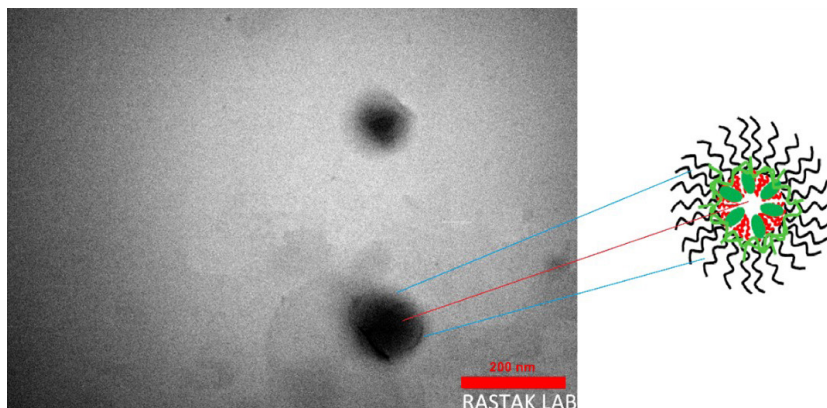


**Figure 1.** TEM of PTX-loaded sericin NPs merged with putative core-shell self assemblies structure

### ***In-vitro* release study of PTX loaded sericin NPs**

The release profile study of PTX-loaded sericin NPs, marketed (Abraxane<sup>®</sup>) and free PTX, was shown in Figure 2. In contrast to Abraxane<sup>®</sup>, which only releases 76% of the medication after the same time, PTX NPs demonstrated a 68% PTX release after 24 h in acidic solutions that mimicked the tumor micro-environment. Because of PTX's strong affinity toward the hydrophobic interior of the NPs, the formulation under study and Abraxane<sup>®</sup> showed a delayed and prolonged release of the drug. The drug included in these NPs may be released gradually owing to their capacity as drug reservoirs<sup>34</sup>. Although the drug release from Abraxane<sup>®</sup> was higher than observed in PTX NPs, both of them had similar release profiles ( $f_2=65$ ). The *in vitro* release profile for free PTX suspension showed only 40% drug release throughout 24 h. The PTX loaded in NPs showed significantly higher release ( $p<0.05$ ) than pure PTX suspension. The calculated similarity factor ( $f_2=36$ ) indicates the difference between these profiles. The elaboration of this result relies on the fact that NPs have a larger surface area compared to the pure drug, which allows for more interactions with the surrounding environment; this, in turn, enhances PTX solubility and thus facilitates faster release of the drug. PTX is known for its poor solubility, but when encapsulated in NPs, it can be enhanced, leading to more efficient release from the NPs<sup>35</sup>.

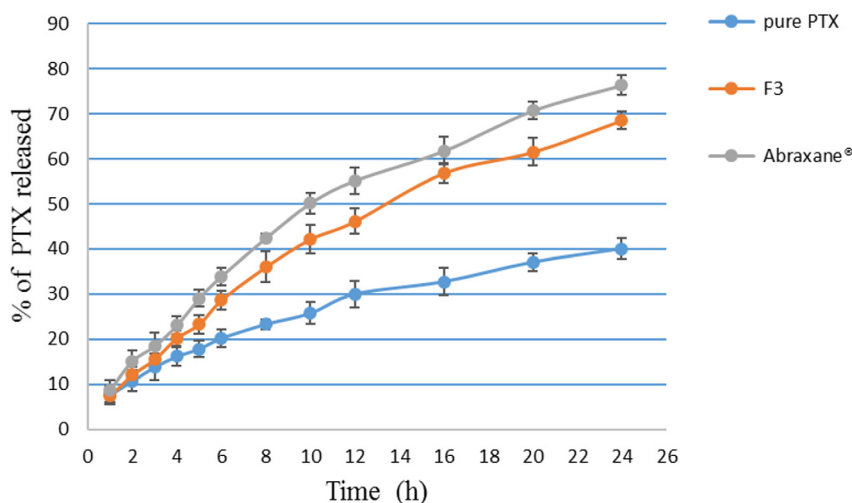


**Figure 2.** *In Vitro*, the release profile of PTX NPs was compared with the marketed product (Abraxane®) and Pure PTX in acetate buffer (pH 5.4) at 37°C.

### ATR-FTIR analysis

FTIR spectroscopy was used to examine the functional group components and structural alterations that occurred during the creation of NPs. Figure 3 displays the IR spectrum of PTX, poloxamer 407, sericin, and the physical combination of PTX, sericin, and poloxamer 407 (1:1:1), and PTX-loaded sericin NPs.

The characteristic peaks in the FTIR spectrum of pure PTX are found at 3400–3500  $\text{cm}^{-1}$  (N-H stretching), 3307  $\text{cm}^{-1}$  (O-H stretching), 1734  $\text{cm}^{-1}$  (C=O) stretching of ester, 1707  $\text{cm}^{-1}$  (C=O) stretching of amide, 1645  $\text{cm}^{-1}$  (C-C) stretching, 1242  $\text{cm}^{-1}$  (C-N) stretching, 1176  $\text{cm}^{-1}$  (NC-O) stretching, and 1072  $\text{cm}^{-1}$  (C-O) stretching<sup>36</sup>. The spectrum of poloxamer 407 shows a band at 2881  $\text{cm}^{-1}$  (C–H) stretching vibration, a band at 1467  $\text{cm}^{-1}$  (C–H) bending vibration, and its distinctive band at 1109  $\text{cm}^{-1}$  (C-O) stretching<sup>37</sup>. Sericin showed characteristic bands of C=O stretching at 1649  $\text{cm}^{-1}$  and N-H bending at 1539  $\text{cm}^{-1}$  of amides I and II, respectively, and broadband peaked at 3342  $\text{cm}^{-1}$  owing to the stretching of the N-H bond of amides in conjunction with the absorption of the O-H groups<sup>38</sup>. The majority of the distinctive peaks for both the drug and the protein were visible in the physical mix spectrum: PTX: sericin: poloxamer 407 at a ratio of 1:1:1, suggesting that there was no drug-excipient interaction. The absence of all the primary peaks in the FT-IR spectrum of the optimum PTX-loaded sericin NP formulation is caused by PTX becoming entrapped in the self-assembled sericin-based PTX NPs. The following bands, which correspond to the properties of poloxamer 407, were seen in the optimized for-

mulation: a band at  $2883\text{ cm}^{-1}$  from C-H stretching vibration, a band at  $1467\text{ cm}^{-1}$  from C-H bending vibration, and a distinctive band at  $1112\text{ cm}^{-1}$  from C-O stretching. In addition, while they have moved to higher wavenumbers  $1647$  and  $1535\text{ cm}^{-1}$ , respectively—the distinctive bands of the sericin N-H bond of amides  $3362\text{ cm}^{-1}$ , amide I, and II are still discernible, indicating the existence of the protein in the structure of the NPs.

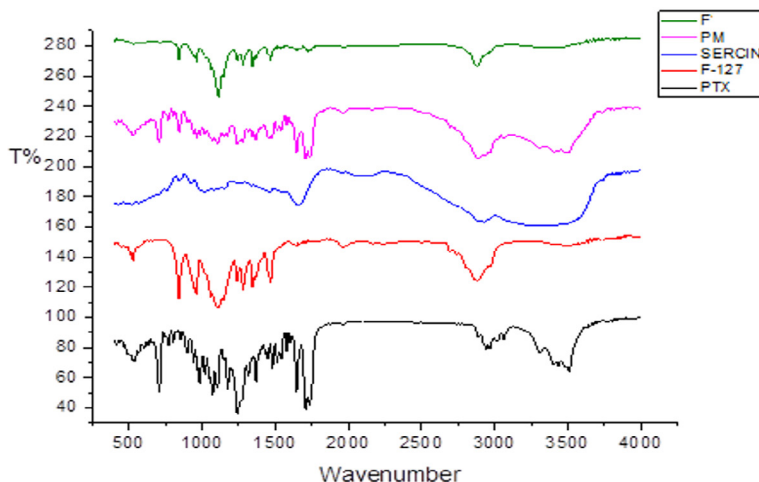


**Figure 3.** FTIR absorption spectrum of pure PTX, sericin, poloxamer 407, physical mixture, and optimized formulation

### DSC analysis

The thermal analysis of PTX-loaded sericin NPs is shown in Figure 4. The DSC profile of PTX shows an endothermic effect at  $T_{\text{peak}} = 220^{\circ}\text{C}$  due to melting, indicating its pure crystalline state<sup>39</sup>. The DSC profile of poloxamer 407 also shows an endothermic effect at  $T_{\text{peak}} = 60^{\circ}\text{C}$  due to melting<sup>40</sup>. The DSC profile of sericin shows a broad endothermic effect at  $T_{\text{peak}} = 122^{\circ}\text{C}$  associated with order  $\rightarrow$  disorder transitions, which can be considered thermal signatures of protein (irreversible) denaturation<sup>41</sup>.

DSC profile of PTX-loaded sericin NPs shows the endothermic peaks of poloxamer 407 and sericin (shifted to lower melting temperatures) due to the presence of the other excipients with an additional peak of mannitol (added as a cryoprotectant) at  $T_{\text{peak}} = 157^{\circ}\text{C}$ . Conversely, there was no peak for PTX at  $122^{\circ}\text{C}$ , suggesting that PTX undergoes conversion to amorphous form (molecularly dispersed) during formulation<sup>42</sup>. These effects in the DSC curve of PTX-loaded sericin NPs confirm the presence of the protein in the structure of NPs.

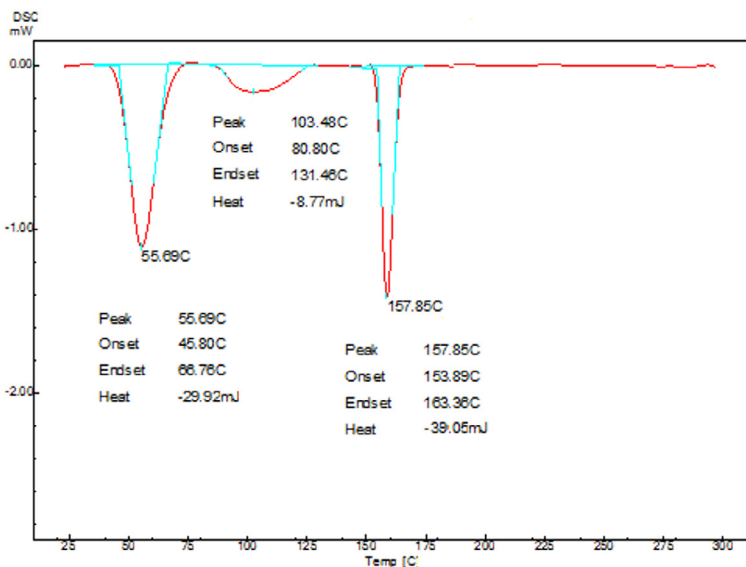


**Figure 4.** DSC profile of PTX-loaded sericin NPs

### ***In-vitro* aerosol dispersion performance by the Next Generation Impactor™**

Nebulizers that can deliver formulations as minute droplets that will be deposited in the lung airways based on their aerodynamic qualities, such as MMAD and FPF, can be used in the pulmonary route of administration. These aerodynamic characteristics of nebulized particles reflect the *in vivo* deposition profile in the alveolar portion of deep lung regions and the airways<sup>43</sup>.

The aerosol dispersion properties of PTX-loaded sericin NPs were evaluated using the Next Generation Impactor™ (NGI™) coupled with the Omron NE-U780 (Omron Healthcare UK Ltd, UK) nebulizer device. They are presented in Figure 5 and Table 1.

The data obtained indicated that the particle size distribution's normalcy, as shown by the MMAD (3.72µm) and GSD (2.06µm), was within the optimal range for pulmonary administration (1–5 and 1–3µm, respectively)<sup>27</sup>. The loaded dose in the device was emitted by an average extent of 81.5%, the average FPF% was about 54.83%, and the average RF% was 74.26%.

**Table 1.** Aerodynamic properties of PTX-loaded sericin NPs

Formulation	MMAD ( $\mu\text{m}$ )	GSD ( $\mu\text{m}$ )	FPF%	RF%	ED%
PTX-NPs	$3.72 \pm 1.08$	$2.06 \pm 0.85$	$54.83 \pm 2.05$	$74.26 \pm 2.96$	$81.50 \pm 2.23$

It is expected that the particles on Stages 5-7, which had significant particle deposition and aerodynamic diameter values of less than  $1 \mu\text{m}$ , would deposit in the deep lung alveolar region through a mechanism of deposition known as diffusion, or Brownian motion. The particles deposited on Stages 1-4 would primarily deposit through sedimentation owing to gravity settling in the middle-to-deep lung regions.

The hydrophilic polymer in the NPs' outer shell and the smallest particle size of PTX-loaded sericin NPs allowed for a repulsive steric interaction between the particles, effectively decreasing the overall adhesive forces. This allowed for more effective aerosolization and stabilization of the colloidal suspension in the air, which allowed the NPs to reach deeper stages of the NGITM device<sup>44</sup>.

NPs that demonstrate the best in-vitro aerosol lung deposition can be inhaled to facilitate local delivery of PTX to the deep lungs. This allows the NPs to deposit in almost all lung regions, allowing for treatment of the entire tissue and minimizing adverse events and exposure to other organs.

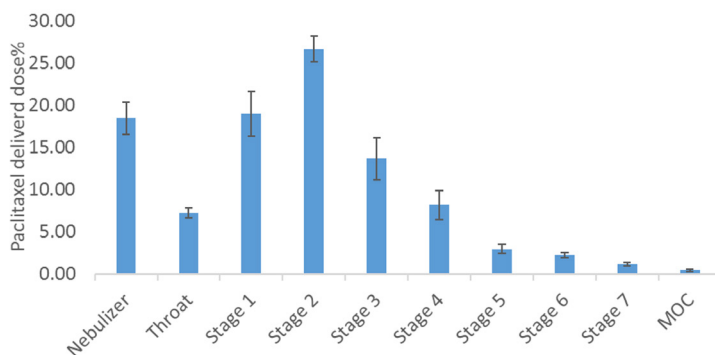


**Figure 5.** The aerosol dispersion performance of the nebulized NPs as the % deposition on each NGITM stage

### ***In-vitro* cytotoxicity**

The MTT assay was used to examine and compare the *in vitro* cytotoxicity of PTX-loaded sericin NPs with that of unloaded blank NPs and free PTX using the human lung cancer cell line A-549. As demonstrated in Figure 6, no significant ( $p > 0.05$ ) cytotoxic activity was seen for the drug-free NPs at dif-

ferent concentrations compared to others, suggesting that the synthetic blank NPs are harmless in cell culture. At all concentrations used (0.1-30 nM), PTX-loaded sericin NPs significantly ( $p < 0.05$ ) outperform pure PTX and blank NPs in terms of cytotoxicity on the A-549 cancer cell line 72 hours after exposure. This indicates that the cells can cleave PTX, allowing the freed PTX to reduce cellular viability. PTX-loaded sericin NPs can enter cancer cells by endocytosis and avoid the efflux pumps that cause PTX therapeutic resistance, which is one reason for their superiority over free PTX. Moreover, unlike free PTX, which clears out quickly, PTX-loaded nanoparticles can release the drug gradually and maintain therapeutic levels for more time. Its continuous release profile may improve the medication's ability to kill cancer cells<sup>45</sup>.

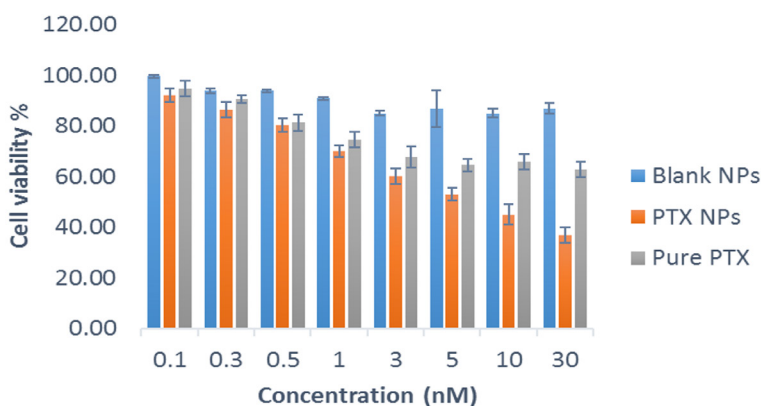


**Figure 6.** Viability of A-549 cells after 72 h of cell culture with different concentrations of PTX

It successfully manufactured PTX-loaded sericin NPs using desolvation and related dialysis processes with spherical morphology of the particles, the lack of particle aggregation, and the core-shell structure with a consistent surface charge. When compared to the reference PTX, it had extended-release behavior. DSC analysis revealed that PTX was amorphous, and FTIR data showed no chemical interaction with the excipients. These particles improved PTX *in vitro* cytotoxicity on lung cancer cells and demonstrated strong aerosol performance *in vitro*. According to the physicochemical and *in vitro* evaluation findings, NPs of PTX have great potential as a pulmonary delivery mechanism.

### **STATEMENT OF ETHICS**

This study does not require ethical permission to be carried out.

### **CONFLICT OF INTEREST STATEMENT**

The authors declare that there are no conflicts of interest regarding the publication of this manuscript.

### **AUTHOR CONTRIBUTIONS**

All authors contributed equally to the article.

### **FUNDING SOURCES**

This research received no specific grant from any funding agency in the public, commercial, or not-for-profit sectors.

### **ACKNOWLEDGMENTS**

The authors thank the Department of Pharmaceutics at the College of Pharmacy Baghdad University for supporting this research article.



## REFERENCES

1. Chhikara BS, Parang K. Global Cancer Statistics 2022: the trends projection analysis. *Chem Biol Lett*, 2023;10(1):451.
2. Cai H, Wang Y, Qin D, Cui Y, Zhang H. Advanced surgical technologies for lung cancer treatment: Current status and perspectives, *Eng Regen*, 2023;4(1):55-67. Doi: 10.1016/j.engreg.2022.12.001
3. Bhattacharya S. Development of 5-FU loaded poly lactic-co-glycolic acid nanoparticles for lung cancer treatment. *Iraqi J Pharm Sci*, 2022;31(1):130-143. Doi: 10.31351/vol31iss1pp130-143
4. Storti C, Le Noci V, Sommariva M, Tagliabue E, Balsari A, Sfondrini L. Aerosol delivery in the treatment of lung cancer. *Curr Cancer Drug Targets*, 2015;15(7):604-612. Doi: 10.2174/1568009615666150602143751
5. Wauthoz N, Rosière R, Amighi K. Inhaled cytotoxic chemotherapy: clinical challenges, recent developments, and future prospects. *Expert Opin Drug Deliv*, 2021;18(3):333-354. Doi: 10.1080/17425247.2021.1829590
6. Sharifi-Rad J, Quispe C, Patra JK, Singh YD, Panda MK, Das G, et al. Paclitaxel: application in modern oncology and nanomedicine-based cancer therapy. *Oxid Med Cell Longev*, 2021;2021:3687700. Doi: 10.1155/2021/3687700
7. Nasser ST, Abdulrassol A, Ghareeb M. Design, preparation and *in-vitro* evaluation of novel ocular antifungal nanoemulsion using posaconazole as a model drug. *Technology*, 2021;11(3):1-7. Doi: 10.25258/ijddt.11.3.00
8. Rosière R, Van Woensel M, Mathieu V, Langer I, Mathivet T, Vermeersch M, et al. Development and evaluation of well-tolerated and tumor-penetrating polymeric micelle-based dry powders for inhaled anticancer chemotherapy. *Int J Pharm*, 2016;501(1-2):148-159. Doi: 10.1016/j.ijpharm.2016.01.073
9. Huang L, Tao K, Liu J, Qi C, Xu L, Chang P, et al. Design and fabrication of multifunctional sericin nanoparticles for tumor targeting and pH-responsive subcellular delivery of cancer chemotherapy drugs. *ACS Appl Mater Interfaces*, 2016;8(10):6577-6585. Doi: 10.1021/acsami.5b11617
10. Seo S-J, Das G, Shin H-S, Patra JK. Silk sericin protein materials: characteristics and applications in food-sector industries. *Int J Mol Sci*, 2023;24(5):4951. Doi: 10.3390/ijms24054951
11. Mandal BB, Kundu S. Self-assembled silk sericin/poloxamer nanoparticles as nano-carriers of hydrophobic and hydrophilic drugs for targeted delivery. *Nanotechnology*, 2009;20(35):355101. Doi: 10.1088/0957-4484/20/35/355101
12. Toma NM, Abdulrasool AA. Formulation and evaluation of montelukast sodium nanoparticles for transdermal delivery. *Int J Drug Deliv Technol*, 2021;11(2):530-538.
13. Ali HH, Hussein AA. Oral nanoemulsions of candesartan cilexetil: formulation, characterization and *in vitro* drug release studies. *AAPS Open*, 2017;3(4):1-16. Doi: 10.1186/s41120-017-0016-7
14. Al-Sawaf OF, Jalal F. Novel probe sonication method for the preparation of meloxicam bilosomes for transdermal delivery: part one. *J Res Med Dent Sci*, 2023;11(6):5-12.
15. Salih O, Muhammed E. Preparation, evaluation, and histopathological studies of ondansetron-loaded invasomes transdermal gel. *J Res Pharm*, 2024;28(1):289-303. Doi: 10.29228/jrp.696

16. Wu Z, Zou X, Yang L, Lin S, Fan J, Yang B, et al. Thermosensitive hydrogel used in dual drug delivery system with Paclitaxel-loaded micelles for *in situ* treatment of lung cancer. *Colloids Surf B Biointerfaces*, 2014;122:90-98. Doi: 10.1016/j.colsurfb.2014.06.052
17. Abdulqader AA, Rajab NA. Preparation and characterization of posaconazole as a nanomicelles using d- $\alpha$ -tocopheryl polyethylene glycol 1000 succinate (TPGS). *Iraqi J Pharm Sci*, 2023;32(Suppl.):26-32. Doi: 10.31351/vol32issSuppl.pp26-32
18. Jasim IK, Abd Alhammid SN, Abdulasool AA. Synthesis and evaluation of B-cyclodextrin based nanosponges of 5-Fluorouracil by using ultrasound assisted method. *Iraqi J Pharm Sci*, 2020;29(2):88-98. Doi: 10.31351/vol29iss2pp88-98
19. Abdullah TM, Al-Kinani KK. Topical propranolol hydrochloride nanoemulsion: a promising approach drug delivery for infantile hemangiomas. *Iraqi J Pharm Sci*, 2023;32:300-315. Doi: 10.31351/vol32issSuppl.pp300-315
20. Li X, Vogt FG, Hayes D Jr, Mansour HM. Design, characterization, and aerosol dispersion performance modeling of advanced spray-dried microparticulate/nanoparticulate mannitol powders for targeted pulmonary delivery as dry powder inhalers. *J Aerosol Med Pulm Drug Deliv*, 2014;27(2):81-93. Doi: 10.1089/jamp.2013.1078
21. Meenach SA, Anderson KW, Hilt JZ, McGarry RC, Mansour HM. High-performing dry powder inhalers of Paclitaxel DPPC/DPPG lung surfactant-mimic multifunctional particles in lung cancer: physicochemical characterization, *in vitro* aerosol dispersion, and cellular studies. *AAPS PharmSciTech*, 2014;15(6):1574-1587. Doi: 10.1208/s12249-014-0182-z
22. Faramarzi P, Haririan I, Ghanbarzadeh S, Yaqoubi S, Hamishehkar H. Development of carrier-free montelukast dry powder inhalation formulation. *Pharm Ind*, 2015;77(10):1535-1542.
23. Meenach SA, Anderson KW, Hilt JZ, McGarry RC, Mansour HM. Characterization and aerosol dispersion performance of advanced spray-dried chemotherapeutic PEGylated phospholipid particles for dry powder inhalation delivery in lung cancer. *Eur J Pharm Sci*, 2013;49(4):699-711. Doi: 10.1016/j.ejps.2013.05.012
24. Boe J, Dennis J, O'Driscoll B, Bauer T, Carone M, Dautzenberg B, et al. European Respiratory Society Guidelines on the use of nebulizers: guidelines prepared by a European Respiratory Society Task Force on the use of nebulizers. *Eur Respir J*, 2001;18(1):228-242. Doi: 10.1183/09031936.01.00220001
25. Katiyar S, Gaur S, Solanki R, Sarangdhar N, Suri J, Kumar R, et al. Indian guidelines on nebulization therapy. *Indian J Tuberc*, 2022;69(Suppl.):1-191. Doi: 10.1016/j.ijtb.2022.06.004
26. Sahib MN, Abdulameer SA, Darwis Y, Peh KK, Tan YTF. Solubilization of beclomethasone dipropionate in sterically stabilized phospholipid nanomicelles (SSMs): physicochemical and *in vitro* evaluations. *Drug Des Devel Ther*, 2012;6:29-42. Doi: 10.2147/DDDT.S28265
27. Shieh-zadeh F, Tafaghodi M, Dehghani ML, Mashhoori F, Bazzaz BSF, Imenshahidi M. Preparation and characterization of a dry powder inhaler composed of PLGA large porous particles encapsulating gentamicin sulfate. *Adv Pharm Bull*, 2019;9(2):255-265. Doi: 10.15171/apb.2019.029
28. Sahib MN, Darwis Y, Peh KK, Abdulameer SA, Tan YTF. Rehydrated sterically stabilized phospholipid nanomicelles of budesonide for nebulization: physicochemical characterization and *in vitro*, *in vivo* evaluations. *Int J Nanomedicine*, 2011;6:2351-2366. Doi: 10.2147/IJN.S25363

29. Salim Al-Khfajy W, Abdulrazzaq MH, Al-Mashhadani Z. Synergistic effects of 2-Deoxy-D-glucose and cinnamic acid with erlotinib on NSCLC cell line. *Iraqi J Pharm Sci*, 2023;32(Suppl.):136-144. Doi: 10.31351/vol32issSuppl.pp136-144
30. Jiménez-López J, Bravo-Caparrós I, Cabeza L, Nieto FR, Ortiz R, Perazzoli G, et al. Paclitaxel antitumor effect improvement in lung cancer and prevention of the painful neuropathy using large PEGylated cationic liposomes. *Biomed Pharmacother*, 2021;133:111059. Doi: 10.1016/j.biopha.2020.111059
31. Akram S, Al-Shammari AM, Sahib HB, Jabir MS. Papaverine enhances the oncolytic effects of Newcastle disease virus on breast cancer *in vitro* and *in vivo*. *Int J Microbiol*, 2023;3324247. Doi: 10.1155/2023/3324247
32. Gill KK, Nazzal S, Kaddoumi A. Paclitaxel-loaded PEG<sub>5000</sub>-DSPE micelles as a pulmonary delivery platform: formulation characterization, tissue distribution, plasma pharmacokinetics, and toxicological evaluation. *Eur J Pharm Biopharm*, 2011;79(2):276-284. Doi: 10.1016/j.ejpb.2011.04.017
33. Carissimi G, Lozano-Pérez AA, Montalbán MG, Aznar-Cervantes SD, Cenis JL, Villora G. Revealing the influence of the degumming process in the properties of silk fibroin nanoparticles. *Polymers*, 2019;11(12):2045. Doi: 10.3390/polym11122045
34. Al-Edhari GH, Al Gawhari FJ. Study the effect of formulation variables on preparation of nisoldipine-loaded nano bilosomes. *Iraqi J Pharm Sci*, 2023;32(Suppl.):271-282. Doi: 10.31351/vol32issSuppl.pp271-282
35. Averineni RK, Shavi GV, Gurram AK, Deshpande PB, Arumugam K, Maliyakkal N, et al. PLGA 50:50 nanoparticles of Paclitaxel: development, *in vitro* antitumor activity in BT-549 cells and *in vivo* evaluation. *Bull Mater Sci*, 2012;35:319-326. Doi: 10.1007/s12034-012-0313-736
36. Pedro IDR, Almeida OP, Martins HR, de Alcântara Lemos J, de Barros ALB, Leite EA, et al. Optimization and *in vitro/in vivo* performance of Paclitaxel-loaded nanostructured lipid carriers for breast cancer treatment. *J Drug Deliv Sci Technol*, 2019;54:101370. Doi: 10.1016/j.jddst.2019.101370
37. Alkufi HK, Kassab HJ. Formulation and evaluation of sustained-release sumatriptan mucoadhesive intranasal in-situ gel. *Iraqi J Pharm Sci*, 2019;28(2):95-104. Doi: 10.31351/vol28iss2pp95-104
38. Saha J, Mondal M, Sheikh MK, Habib M. Extraction, structural and functional properties of silk sericin biopolymer from *Bombyx mori* silk cocoon waste. *J Text Sci Eng*, 2019;9(2). Doi: 10.4172/2165-8064.1000390
39. Jangid AK, Pooja D, Jain P, Gupta N, Ramesan S, Kulhari H. Self-assembled and pH-responsive polymeric nanomicelles impart effective delivery of Paclitaxel to cancer cells. *RSC Adv*, 2021;11(23):13928-13999. Doi: 10.1039/D1RA01574E
40. Al Khalidi MM, Jawad FJ. Enhancement of aqueous solubility and dissolution rate of etoricoxib by solid dispersion technique. *Iraqi J Pharm Sci*, 2020;29(1):76-87. Doi: 10.31351/vol29iss1pp76-87
41. Balcão VM, Harada LK, Jorge LR, Oliveira JM Jr, Tubino M, Vila MM. Structural and functional stabilization of sericin from *Bombyx mori* cocoons in a biopolysaccharide film: bioorigami for skin regeneration. *J Braz Chem Soc*, 2020;31(4):833-848. Doi: 10.21577/0103-5053.20190247

42. Eglar M, Hammid S. Design of zolmitriptan liquisolid orodispersible tablets and their *in vitro* evaluation. *J Chem Pharm Res*, 2016;8(11):232-242. Doi: 10.22159/ijpps.2017v9i1.15656
43. Elbatanony RS, Parvathaneni V, Kulkarni NS, Shukla SK, Chauhan G, Kunda NK, et al. Afatinib-loaded inhalable PLGA nanoparticles for localized therapy of non-small cell lung cancer (NSCLC) development and *in-vitro* efficacy. *Drug Deliv Transl Res*, 2021;11:927-943. Doi: 10.1007/s13346-020-00802-8
44. Sahib MN, Darwis Y, Khiang PK, Tan YTF. Aerodynamic characterization of marketed inhaler dosage forms: high-performance liquid chromatography assay method for the determination of budesonide. *Afr J Pharm Pharmacol*, 2010;4(12):878-884.
45. Song RF, Li XJ, Cheng XL, Fu AR, Wang YH, Feng YJ, et al. Paclitaxel-loaded trimethyl chitosan-based polymeric nanoparticles for the effective treatment of gastrointestinal tumors. *Oncol Rep*, 2014;32(4):1481-1488. Doi: 10.3892/or.2014.3344